Invariant set-based analysis of minimal detectable fault for discrete-time LPV systems with bounded uncertainties

Junbo Tan, Sorin Olaru, Monica Roman, Feng Xu, Bin Liang

IEEE Access
Multidisciplinary | Rapid Review | Open Access Journal

Received September 18, 2019, accepted October 8, 2019, date of publication October 18, 2019, date of current version October 31, 2019.

Digital Object Identifier 10.1109/ACCESS.2019.2948362

Invariant Set-Based Analysis of Minimal Detectable Fault for Discrete-Time LPV Systems With Bounded Uncertainties

JUNBO TAN[1,2], (Student Member, IEEE), SORIN OLARU[2], (Senior Member, IEEE), MONICA ROMAN[3], FENG XU[4], AND BIN LIANG[1]

[1]Tsinghua National Laboratory for Information Science and Technology, Tsinghua University, Beijing 100084, China
[2]Laboratory of Signals and Systems, Universityof Paris-Sud-CentraleSupelec-CNRS, Université Paris Saclay, 91190 Paris, France
[3]Department of Automation and Electronics, University of Craiova, 200585 Craiova, Romania
[4]Center for Artificial Intelligence and Robotics, Tsinghua Shenzhen International Graduate School, Tsinghua University, Shenzhen 518055, China

Corresponding authors: Sorin Olaru (sorin.olaru@centralesupelec.fr) and Feng Xu (xu.feng@sz.tsinghua.edu.cn)

This work was supported in part by the Romanian Ministry of Research and Innovation, CNCS-UEFISCDI, under Project PN-III-P1-1.1-TE-2016-0862, in part by the MOSCBIOS through the PNCDI III, in part by the National Natural Science Foundation of China under Grant U1813216, and in part by the Basic Research Program of Shenzhen under Grant JCYJ20170817152701660 and Grant JCYJ20160301100921349.

ABSTRACT This paper proposes an invariant-set based minimal detectable fault (MDF) computation method based on the set-separation condition between the healthy and faulty residual sets for discrete-time linear parameter varying (LPV) systems with bounded uncertainties. First, a novel invariant-set computation method for discrete-time LPV systems is developed exclusively based on a sequence of convex-set operations. Notably, this method does not need to satisfy the existence condition of a common quadratic Lyapunov function for all the vertices of the parametric uncertainty compared with the traditional invariant-set computation methods. Based on asymptotic stability assumptions, a family of robust positively invariant (RPI) outer-approximations of minimal robust positively invariant (mRPI) set are obtained by using a shrinking procedure. Based on the mRPI set, the healthy and faulty residual sets can be obtained. Then, by considering the dual case of the set-separation constraint regarding the healthy and faulty residual sets, we transform the guaranteed MDF problem based on the set-separation constraint into a simple linear programming (LP) problem to compute the magnitude of MDF. Since the proposed MDF computation method is robust regardless of the value of scheduling variables in a given convex set, fault detection (FD) can be guaranteed whenever the magnitude of fault is larger than that of the MDF. At the end of the paper, a practical vehicle model is used to illustrate the effectiveness of the proposed method.

INDEX TERMS Invariant set, minimum detectable fault, LPV systems.

I. INTRODUCTION

Fault diagnosis has attracted much attention from a great number of researchers owing to the demand of increasing safety and reliability of the modern industrial control systems. Fault occurrence affects the behavior of the system and prevents it from operating in a normal way [3]. The objective of fault diagnosis is to detect, isolate, identify or estimate faults after they have affected the system behaviors. FD determines whether a fault has occurred or not in a system, fault isolation finds the system component where the fault has occurred and fault identification or estimation determines the fault type and magnitude [25].

As a kind of important set-based FD method, the feature of the invariant-set technique consists in testing consistency between the measured real-time residual signals and the reference residual set generated from the nominal models. In particular, as long as the system is healthy, the residual signal will always stay inside the healthy residual set at steady stage. Whenever faults occur in the system, the residual signal will violate the frontiers of the healthy residual set and finally enter into the faulty residual set [20], [21]. Thus, as long as

The associate editor coordinating the review of this manuscript and approving it for publication was Baoping Cai.

the healthy and faulty residual sets are separated from each other, it is guaranteed that the occurred fault can be detected in the steady stage.

The core of invariant set-based FD consists in the construction of the healthy and faulty invariant sets. For linear time-invariant (LTI) systems with bounded uncertainties, the technique on the computation of the invariant set is relatively mature. A stand tool for ultimate invariant set computation is by using the Lyapunov function, whose sublevel sets are positively invariant and their shapes can be used to characterize the steady behaviors of system dynamics [9]. Reference [10] developed a systematic method to obtain the robust positively invariant (RPI) sets for both continuous-time and discrete-time perturbed LTI systems from the aspect of component-wise analysis, which can decrease the conservatism of invariant sets and improve the state-estimation precision to some extent. In [7], the attractive ellipsoid method was extended to guarantee the convergence of state trajectories to the origin and simultaneously minimize the size of an ellipsoidal set despite the presence of non-vanishing disturbances.

However, the results on the computation of invariant sets for LPV systems are limited. This class of dynamical systems serve as a bridge connecting linear and nonlinear systems [23] and could be handled by using some techniques for linear systems at each operating point [4], [22]. Reference [16] developed an ellipsoidal invariant set computation method to maximize the inclusion of a given reference direction by considering additive disturbances injected into the system dynamics. Reference [14] used an H_∞ observer and linear matrix inequalities (LMIs) to compute an RPI set, whose evolution is characterized to bound the estimation error at each time instant. However, regarding both methods in [14] and [16], there is a precondition that a common quadratic Lyapunov function for all vertex matrices of LPV systems should exist, which is a strict assumption and not a necessary one for stable LPV systems. In addition, [19] presented a component-wise based RPI set computation method for polytopic uncertain systems, which does not rely on the existence of common quadratic Lyapunov functions while needs to search a common invertible transformation matrix to guarantee the Schur stability. Unfortunately, this searching process is a non-convex problem and a numerical search routine, which is not easy to implement, is needed.

For linear discrete-time systems affected by bounded uncertainties, [17] proposed an interesting method to compute an mRPI set by using a contractive procedure starting from an initial RPI set. According to the work [17], we propose a novel and practical mRPI set computation method to characterize the healthy and faulty residual sets of perturbed discrete-time LPV systems exclusively based on a sequence of convex-set operations without need of existence of a common quadratic Lyapunov function assumed in [16] and [14]. Meanwhile, a family of outer-approximations of the mRPI set are obtained by using a shrinking procedure, which are also positively invariant at each step of iteration.

The proposed invariant-set computation method leads to the healthy and faulty residual sets for the discrete-time LPV systems and completes the available methods in the literature [6], [18], [24] based on adaptive thresholds, interval analysis or LMIs. As known, since the sensitivity of FD is highly affected by the system uncertainties, the characterization of MDF is important in order to know the limits of performance of the considered FD scheme. We consider computing the magnitude of MDF based on the set-separation constraint on the healthy and faulty residual sets. By exploiting the duality, we can transform the guaranteed MDF problem into a simple linear programming (LP) problem. Furthermore, we can compute the magnitude of MDF only by solving a simple LP problem and avoid the complex set-based optimization operations. The magnitude of MDF is related to the varying range of scheduling variables. In particular, the larger the varying range of scheduling variables is, the more conservatism the obtained results on the magnitude of MDF have. That means, the magnitude of MDF will increase as the varying range of scheduling variables increases.

For clarity, the main contributions of this paper are summarized as follows:

- A novel invariant set computation method is proposed for discrete-time LPV systems with bounded uncertainties exclusively based on a sequence of convex-set operations. This computation method does not need to satisfy the strict assumption that there exists a common quadratic Lyapunov function for all the vertex matrices of LPV system.
- By considering the duality of set-separation constraint between the healthy and faulty residual sets, we transform the MDF problem into a simple LP problem. The magnitude of MDF for additive actuator and sensor faults can be efficiently computed by solving a simple LP problem.
- The conservatism of results on the magnitude of MDF can be decreased by adjusting the varying range of scheduling variables. The smaller the varying range of scheduling variables is, the smaller the obtained magnitude of MDF for additive actuator faults and sensor faults is.

For the convenience of illustration, we introduce some mathematical symbols. $\mathbb{R}^n$ denotes the set of n-dimensional real numbers. $\|\cdot\|_\infty$ indicates the ∞-norm. For two sets X and Y, the Minkowski sum of X and Y is given by $X \oplus Y = \{z | z = x + y,\ x \in X, y \in Y\}$. A polyhedral set P is defined by its half-space representation, $P = \{x | Hx \leq b\}$. A polytope is a closed polyhedral set.

Regarding the structure of the paper, Section II presents the discrete-time LPV system affected by additive actuator and sensor faults and a stability analysis of the state-estimation error dynamics of the designed FD observer in healthy situation is performed. In Section III, the construction method of the mRPI set for the LPV-form state-estimation error dynamics is proposed. In Section IV, the computation method of MDF for additive actuator faults is proposed by

solving a simple LP problem. Section V further proposes the computation method of MDF for additive sensor faults. A practical vehicle application is used to illustrate the effectiveness of the proposed method in Section VI. Some conclusions are drawn in Section VII.

II. SYSTEM MODEL

This section introduces the class of dynamics under study and the associated family of faults and discusses the stability prerequisites for the state-estimation error dynamics of the designed FD observer in healthy situation.

A. SYSTEM MODEL

Considering the following discrete-time LPV system affected by additive actuator faults:

$$x_{k+1} = A(\theta_k)x_k + B(\theta_k)u_k + Gf_k + Ew_k, \tag{1a}$$
$$y_k = C(\theta_k)x_k + D(\theta_k)u_k + Pg_k + F\eta_k, \tag{1b}$$

where $k \in \mathbb{N}$ is the discrete time index. $A(\theta_k) \in \mathbb{R}^{n_x \times n_x}$, $B(\theta_k) \in \mathbb{R}^{n_x \times n_u}$, $C(\theta_k) \in \mathbb{R}^{n_y \times n_x}$ and $D(\theta_k) \in \mathbb{R}^{n_y \times n_u}$ are related system matrices dependent on a varying scheduling vector $\theta_k \in \mathbb{R}^{n_\theta}$ able to be measured online at time instant k. $x_k \in \mathbb{R}^{n_x}$ and $y_k \in \mathbb{R}^{n_y}$ are the system states and outputs at time instant k, respectively. The unknown inputs $w_k \in \mathbb{R}^{n_w}$ (including process disturbances, modeling errors, etc.) are contained in a known compact and convex set $\mathbf{W} = \{w \in \mathbb{R}^{n_w} | H_w w \leq b_w\}$ containing the origin. Similarly, the measurement noises $\eta_k \in \mathbb{R}^{\eta}$ also belong to a given compact and convex set $\mathbf{V} = \{\eta \in \mathbb{R}^{n_\eta} | H_\eta \eta \leq b_\eta\}$ containing the origin. $f_k \in \mathbb{R}^{n_f}$ and $g_k \in \mathbb{R}^{n_g}$ denote the additive actuator and sensor fault vectors, respectively. $G \in \mathbb{R}^{n_x \times n_f}$, $E \in \mathbb{R}^{n_x \times n_w}$, $P \in \mathbb{R}^{n_y \times n_g}$ and $F \in \mathbb{R}^{n_y \times n_\eta}$ are the known constant distribution matrices of f, w_k, g and η_k, respectively.

It is assumed that the n_θ-dimensional scheduling vector θ_k is a convex combination of given extreme values generating a convex set $\Theta = \mathbf{Conv}\{\theta^1, \theta^2, \ldots, \theta^{\mathcal{N}}\}$. Therefore, a linear affine function $\Phi(\theta_k)$ of θ_k can be written as the convex combination of vertex matrices:

$$\Phi(\theta_k) = \sum_{i=1}^{\mathcal{N}} \lambda_i(\theta_k)\Phi(\theta^i), \tag{2}$$

where the weighting coefficients $\lambda_i(\theta_k)$ satisfy $\sum_{i=1}^{\mathcal{N}} \lambda_i(\theta_k) = 1$, $0 \leq \lambda_i(\theta_k) \leq 1$ and the components of $\Phi(\cdot)$ can represent the elements of $A(\cdot)$, $B(\cdot)$, $C(\cdot)$ and $D(\cdot)$.

B. DESIGN OF FD OBSERVER

In order to implement a robust FD, we consider the following Luenberger-structure observer:

$$\hat{x}_{k+1} = A(\theta_k)\hat{x}_k + B(\theta_k)u_k + L(y_k - \hat{y}_k), \tag{3a}$$
$$\hat{y}_k = C(\theta_k)\hat{x}_k + D(\theta_k)u_k, \tag{3b}$$

where $\hat{x}_k$ and $\hat{y}_k$ are the estimated state and output vectors of the system (1), respectively. $L \in \mathbb{R}^{n_x \times n_y}$ is the gain matrix of the designed FD observer (3).

In the healthy situation without any actuator and sensor fault (i.e., $f = \mathbf{0}$, $g = \mathbf{0}$), the state-estimation error e_k is defined as

$$e_k = x_k - \hat{x}_k. \tag{4}$$

Furthermore, the dynamics of the state-estimation error e_k in the healthy situation can be obtained as

$$e_{k+1} = (A(\theta_k) - LC(\theta_k))e_k + Ew_k - LF\eta_k. \tag{5}$$

Since w_k and η_k are the additive terms in (5) and are contained in the sets $\mathbf{W}$ and $\mathbf{V}$, respectively, the bounded-input, bounded-output (BIBO) stability of the dynamics (5) needs to be assessed. Consider the nominal system:

$$e'_{k+1} = (A(\theta_k) - LC(\theta_k))e'_k. \tag{6}$$

A stability conclusion for the nominal system (6) is presented in Theorem 1.

Theorem 1 ([5]): The dynamics (6) *is poly-quadratically stable if and only if there exist symmetric positive definite matrices S_i, S_j, and matrices M_i of appropriate dimensions such that*

$$\begin{bmatrix} M_i + M_i^T - S_i & * \\ (A_i - LC_i)M_i & S_j \end{bmatrix} \succ 0, \quad \forall i,\ j = 1, 2, \ldots, \mathcal{N}, \tag{7}$$

where the symbol $*$ denotes the transpose of $(A_i - LC_i)M_i$. In this case, the time-varying parameter-dependent Lyapunov function for the stability is given as $V(e'_k, \theta_k) = {e'_k}^T R(\theta_k)e'_k$, with $R(\theta_k) = \sum_{i=1}^{\mathcal{N}} \lambda_i(\theta_k)S_i^{-1}$, $\sum_{i=1}^{\mathcal{N}} \lambda_i(\theta_k) = 1$ and $0 \leq \lambda_i(\theta_k) \leq 1$.

Remark 1: The poly-quadratical stability condition of (6) *is satisfied when the system matrix $A(\theta_k) - LC(\theta_k)$ is linear function of θ_k. Thus, the gain L of FD observer* (3) *is constant when the output matrix $C(\theta_k)$ is scheduled by θ_k. On the contrary, if the output matrix C is constant, in this case, the gain matrix L could be dependent on the scheduling vector θ_k, i.e., $L(\theta_k)$.*

From the structural point of view, the results in [15] provided a link between stability conditions and additional structural properties of Lyapunov functions for the nominal system (6). The necessary and sufficient condition regarding the poly-quadratically stability of the dynamics (6) is equivalent to that there exists a scheduling-variable dependent Lyapunov function $V(e'_k, \theta_k) = {e'_k}^T R(\theta_k)e'_k$ satisfying Theorem 1 which is considerably less conservative than the condition that there exists a common quadratic Lyapunov function for all vertex matrices in [14] and [16]. The subsequent computation of RPI sets assumes the fulfillment of this necessary and sufficient stability condition.

C. ROBUST POSITIVELY INVARIANT SETS

Here we first introduce some basic set invariance notions [8], which are the basis of the proposed approaches in the remaining parts.

Definition 1: A set $\mathbb{E}$ *is a positively invariant (PI) set of the dynamics* $e_{k+1} = (A(\theta_k) - LC(\theta_k))e_k$, *if* $\forall \theta_k \in \Theta$, *for any* $e_k \in \mathbb{E}$, *one has* $e_{k+1} \in \mathbb{E}$.

Definition 2: A set $\mathbb{E}$ *is an RPI set of the dynamics* $e_{k+1} = (A(\theta_k) - LC(\theta_k))e_k + Ew_k - LF\eta_k$, *if* $\forall \theta_k \in \Theta$, $w_k \in \mathbf{W}$ *and* $\eta_k \in \mathbf{V}$, *for any* $e_k \in \mathbb{E}$, *one has* $e_{k+1} \in \mathbb{E}$.

Definition 3: The minimal RPI (mRPI) set of the dynamics is defined as an RPI set contained in any closed RPI set and the mRPI set is unique and compact.

III. SET-THEORETIC ANALYSIS IN HEALTHY SITUATION

This section presents the computation method for the approximation of the mRPI set of the LPV-form state-estimation error dynamics (5). If the condition of Theorem 1 is fulfilled, then the system (6) is asymptotically stable. Moreover, w_k and η_k in the dynamics (5) are bounded, i.e., $w_k \in \mathbf{W}$ and $\eta_k \in \mathbf{V}$. Therefore, there exists a family of RPI sets for the dynamics (5). More information on the relationship between system stability and set invariance can be found in [2].

A. CONVEX HULL OF THE MRPI SET

In general, although the mRPI set of the dynamics (5) is not a convex set [1], the robust positive invariance of the convex hull of the mRPI set for the dynamics (5) can be guaranteed by the following theorem.

Theorem 2: Suppose the dynamics (6) *is stable. Then, the convex hull of the mRPI set of the dynamics* (5) *for arbitrary* $\theta_k \in \Theta$ *is an RPI set.*

Proof: Let $\bar{\Omega}$ denote the mRPI set of the dynamics (5) and the convex hull of $\bar{\Omega}$ is $\Omega_\infty := \mathbf{Conv}\{\bar{\Omega}\}$. Since $\bar{\Omega}$ is the mRPI set of the dynamics (1), based on Definitions 2 and 3, we have

$$\left(\sum_{i=1}^{\mathcal{N}} \lambda_i(\theta_k)(A_i - LC_i)\right) \bar{\Omega} \oplus \mathbf{S} \subseteq \bar{\Omega}, \tag{8}$$

where $\mathbf{S} = E\mathbf{W} \oplus (-LF)\mathbf{V}$. For any $d \in \Omega_\infty$, there exist d_1, $d_2 \in \bar{\Omega}$ and $0 \le \alpha \le 1$, such that $d = \alpha d_1 + (1-\alpha)d_2$. Furthermore,

$$\begin{aligned}
&\sum_{i=1}^{\mathcal{N}} \lambda_i(\theta_k)(A_i - LC_i)d + Ew_k - LF\eta_k \\
&= \sum_{i=1}^{\mathcal{N}} \lambda_i(\theta_k)(A_i - LC_i)\alpha d_1 \\
&\quad + \sum_{i=1}^{\mathcal{N}} \lambda_i(\theta_k)(A_i - LC_i)(1-\alpha)d_2 + Ew_k - LF\eta_k \\
&= \alpha\left(\sum_{i=1}^{\mathcal{N}} \lambda_i(\theta_k)(A_i - LC_i)d_1 + Ew_k - LF\eta_k\right) \\
&\quad + (1-\alpha)\left(\sum_{i=1}^{\mathcal{N}} \lambda_i(\theta_k)(A_i - LC_i)d_2 + Ew_k - LF\eta_k\right).
\end{aligned} \tag{9}$$

Let us note that there exist $\tilde{d}_1, \tilde{d}_2 \in \bar{\Omega}$ such that:

$$\begin{aligned}
\tilde{d}_1 &= \left(\sum_{i=1}^{\mathcal{N}} \lambda_i(\theta_k)(A_i - LC_i)d_1 + Ew_k - LF\eta_k\right), \\
\tilde{d}_2 &= \left(\sum_{i=1}^{\mathcal{N}} \lambda_i(\theta_k)(A_i - LC_i)d_2 + Ew_k - LF\eta_k\right).
\end{aligned}$$

Thus, ultimately we have

$$\begin{aligned}
&\sum_{i=1}^{\mathcal{N}} \lambda_i(\theta_k)(A_i - LC_i)d + Ew_k - LF\eta_k \\
&\qquad = \alpha\tilde{d}_1 + (1-\alpha)\tilde{d}_2 \in \mathbf{Conv}\{\bar{\Omega}\} = \Omega_\infty.
\end{aligned} \tag{10}$$

Based on Definition 2, this implies that Ω_∞ is an RPI set of the dynamics (5). □

Since the convex hull of the mRPI set is the tightest convex set containing the mRPI set of the dynamics (5), its characterization will represent the objective of the present section. In the following, all analyses and computations are based on dealing with Ω_∞, the convex hull of the mRPI set for the dynamics (5). For simplicity, we also denote (with an abuse of notation) Ω_∞ as the mRPI set.

B. COMPUTATION OF AN INITIAL RPI SET

Theorem 3: Under the condition of Theorem 1, consider an arbitrarily given initial convex set $\mathbf{E}_0 \supseteq \Omega_\infty$, *where* Ω_∞ *is the mRPI set of the dynamics* (5). *Let the following set iteration*:

$$\bar{\mathbf{E}}_{k+1} = \mathcal{A}(\mathbf{E}_k) \oplus \mathbf{S}, \tag{11a}$$

$$\mathbf{E}_{k+1} = \mathbf{Conv}\left\{\bar{\mathbf{E}}_{k+1} \bigcup \mathbf{E}_k\right\}, \tag{11b}$$

where $\mathcal{A}(\cdot)$ *is the set mapping:*

$$\mathcal{A}(\mathbf{E}_k) = \mathbf{Conv}\left\{\bigcup_{i=1}^{\mathcal{N}} (A_i - LC_i)\mathbf{E}_k\right\}.$$

There exists a finite $k^* \in \mathbb{N}$ *such that* $\mathbf{E}_{k^*+1} = \mathbf{E}_{k^*}$. *Moreover,* $\mathbf{E}_{k^*}$ *is an RPI set for the dynamics* (5).

Proof: Let us first consider the following sequence

$$\tilde{\mathbf{E}}_{k+1} = \mathcal{A}(\tilde{\mathbf{E}}_k) \oplus \mathbf{S}. \tag{12}$$

For a stable dynamics (5), if $\tilde{\mathbf{E}}_0 \supseteq \Omega_\infty$, then there exists a specific positive k^* such that $\tilde{\mathbf{E}}_k \subseteq \tilde{\mathbf{E}}_0$, $\forall k \ge k^*$ as long as the system is stable and for any initial condition in $\tilde{\mathbf{E}}_0$, the state trajectories reach in finite time a neighborhood of Ω_∞. Notice that

$$\mathbf{E}_k = \mathbf{Conv}\left\{\bigcup_{i=0}^{k} \tilde{\mathbf{E}}_i\right\}, \tag{13}$$

with $\tilde{\mathbf{E}}_0 = \mathbf{E}_0$, which is a convex set. For $k = k^*+1$, we have

$$\mathbf{E}_{k^*+1} = \mathbf{Conv}\left\{\mathbf{E}_{k^*} \bigcup \tilde{\mathbf{E}}_{k^*+1}\right\}. \tag{14}$$

Since $\tilde{\mathbf{E}}_{k^*+1} \subseteq \tilde{\mathbf{E}}_0 \subseteq \mathbf{E}_{k^*}$, we have $\mathbf{E}_{k^*+1} = \mathbf{Conv}\left\{\mathbf{E}_{k^*} \bigcup \tilde{\mathbf{E}}_{k^*+1}\right\} = \mathbf{E}_{k^*}$.

Thus, according to (11b), we can further obtain

$$\mathbf{E}_{k^*} = \mathbf{Conv}\left\{\bar{\mathbf{E}}_{k^*+1} \bigcup \mathbf{E}_{k^*}\right\},$$

which indicates that $\bar{\mathbf{E}}_{k^*+1} \subseteq \mathbf{E}_{k^*}$ holds. By combining (11a) and (11b), we can further obtain

$$\bar{\mathbf{E}}_{k^*+1} = \mathcal{A}(\mathbf{E}_{k^*}) \oplus \mathbf{S} \subseteq \mathbf{E}_{k^*}. \tag{15}$$

If $e_k \in \mathbf{E}_{k^*}$, then

$$e_{k+1} = \sum_{i=1}^{\mathcal{N}} \lambda_i(\theta_k)(A_i - LC_i)e_k + Ew_k - LF\eta_k \in \mathcal{A}(\mathbf{E}_{k^*}) \oplus \mathbf{S} \subseteq \mathbf{E}_{k^*}. \tag{16}$$

and thus $\mathbf{E}_{k^*}$ is a convex RPI set for the dynamics of (5). □

Remark 2: If the initial set $\mathbf{E}_0$ is contained in the mRPI set Ω_∞, i.e., $\mathbf{E}_0 \subseteq \Omega_\infty$, then the existence of finite k^* such that $\mathbf{E}_{k^*+1} = \mathbf{E}_{k^*}$ can not be guaranteed. In this case, $\mathbf{E}_k$ is not an RPI set at any iteration and only represents an inner approximation of the mRPI set of the dynamics (5)*. For further details, readers can refer the work in [11].*

Remark 3: We compute the convex hull twice in Theorem 3, i.e., (11a) *and* (11b)*. Obviously,* $\mathbf{Conv}\{\cdot\}$ *in* (11a) *is used to compute the one-step reachable set. We must point out that the significance of* $\mathbf{Conv}\{\cdot\}$ *operation in* (11b) *allows to preserve the convexity of the set iterations. However, the convexity comes at the price of monotonic increasing as long as* $\mathbf{E}_{k+1} \supseteq \mathbf{E}_k$.

The alternative procedures in [16] and [14] use LMI conditions to construct an RPI set under the precondition that there exists a common quadratic Lyapunov function for all vertex matrices of LPV system. Here we provide a more practical way to construct an RPI set based exclusively on convex operators over sets. Moreover, if $\mathbf{E}_0$, $\mathbf{W}$ and $\mathbf{V}$ are polyhedral sets, then (11a) and (11b) provide a sequence of polyhedral sets and $\mathbf{E}_{k^*}$ is polyhedral. Next we will be concerned with the shrinking of a given RPI set in order to better outer approximate the mRPI set and iteratively converge towards the mRPI set by following the idea in [17].

C. SHRINKING PROCEDURE

Considering that the unknown inputs w_k and the measurement noises η_k are both bounded by the known convex sets, i.e., $w_k \in \mathbf{W}$ and $\eta_k \in \mathbf{V}$, we can recursively build a sequence of RPI sets starting with the initial RPI set $\mathbf{E}_{k^*}$ according to the following theorem.

Theorem 4: Given an initial RPI set $\mathbf{E}_{k^*}$ for (5)*, the sequence Ω_k:*

$$\Omega_{k+1} = \mathcal{A}(\Omega_k) \oplus \mathbf{S}, \tag{17}$$

with $\Omega_0 = \mathbf{E}_{k^*}$, ensures that at each iteration Ω_k is an RPI set of (5) *and*

$$\Omega_\infty \subseteq \Omega_{k+1} \subseteq \Omega_k \subseteq \Omega_0 \tag{18}$$

holds for $k \geq 1$. Furthermore, we have

$$\Omega_\infty = \lim_{k \to +\infty} \Omega_k = \bigoplus_{i=0}^{\infty} \mathcal{A}^i(\mathbf{S}), \tag{19}$$

which is the exact mRPI set of the dynamics (5)*.*

Proof: Suppose that $\Omega_0 = \mathbf{E}_{k^*}$ is an RPI set of the dynamics (5). Ω_1 can be computed as

$$\Omega_1 = \mathcal{A}(\Omega_0) \oplus \mathbf{S}, \tag{20}$$

which characterizes the set of all possible e_1 starting from the initial $e_0 \in \Omega_0$. Since Ω_0 is an RPI set, we have

$$\Omega_1 \subseteq \Omega_0. \tag{21}$$

Furthermore, by considering $\Omega_{k+1} \subseteq \Omega_k$, we can obtain

$$\Omega_{k+2} = \mathcal{A}(\Omega_{k+1}) \oplus \mathbf{S} \subseteq \mathcal{A}(\Omega_k) \oplus \mathbf{S} = \Omega_{k+1}, \tag{22}$$

which means that all e_{k+1} starting from Ω_{k+1} will evolve into $\Omega_{k+2} \subseteq \Omega_{k+1}$. Thus, Ω_{k+1} is also an RPI set. Thus, Ω_k describes a monotonic sequence (in terms of set inclusions) of RPI sets. This is lower bounded by the mRPI set which is contained in any RPI set by definition. The monotonic and lower bounded sequence is thus convergent. In order to prove that the limit set Ω_∞ is the mRPI set and not only an RPI set, it should be noted that

$$\Omega_\infty = \mathcal{A}(\Omega_\infty) \oplus \mathbf{S} \tag{23}$$

and $\Omega_{k+1} \subseteq \Omega_k$ whenever $\Omega_k \neq \Omega_\infty$. Exploiting the fact that the mRPI set is known to be unique and to verify (23), we can obtain that Ω_∞ is the mRPI set of dynamics (5). Furthermore, the recursive equation (17) can be written in a more explicit way by iterating from Ω_0. Thus, a polyhedral RPI set is obtained as follows:

$$\Omega_k = \mathcal{A}^k(\Omega_0) \oplus \sum_{i=1}^{k} \mathcal{A}^{i-1}(\mathbf{S}). \tag{24}$$

Considering $\lim_{k \to +\infty} \mathcal{A}^k(\Omega_0) = \mathbf{0}$, it follows (19). □

As pointed out in Remark 2, we should find a proper $\mathbf{E}_0$ such that $\Omega_\infty \subseteq \mathbf{E}_0$ holds. Considering that the mRPI set Ω_∞ is convex, unique and compact, we can always find a proper $\mathbf{E}_0$ such that $\Omega_\infty \subseteq \mathbf{E}_0$. We will propose a practical method to compute the proper set $\mathbf{E}_0$ in the following Theorem 5.

Theorem 5: Suppose that the dynamics (5) *is stable, the initial convex set $\mathbf{E}_0 \supseteq \Omega_\infty$ can be given by*

$$\mathbf{E}_0 = \bigoplus_{i=0}^{p^*-1} \mathcal{A}^i(\mathbf{B}(r)) \oplus \frac{p^*\xi}{1-\xi}\mathbf{B}(r), \tag{25}$$

where $\xi \in (0,1)$, $p^* \in \mathbb{N}$ and $\mathbf{B}(r) := \{x \in \mathbb{R}^{n_x} : \|x\|_\infty \leq r\}$ is a box containing $\mathbf{S}$.

Proof: Since the dynamics (5) is stable, it implies that there exist a scalar $\xi \in (0,1)$, $p^* \in \mathbb{N}$ and a box $\mathbf{B}(r)$ containing $\mathbf{S}$, i.e., $\mathbf{S} \subseteq \mathbf{B}(r)$, such that for any $k \geq p^*$, $\mathcal{A}^k(\mathbf{B}(r)) \subseteq \xi\mathbf{B}(r)$. Moreover, assuming for any $k \geq np^*$,

$\mathcal{A}^k(\mathbf{B}(r)) \subseteq \xi^n\mathbf{B}(r)$ holds for a given n, then for any $k \geq (n+1)p^*$,

$$\begin{aligned}\mathcal{A}^k(\mathbf{B}(r)) &= \mathcal{A}^{p^*}(\mathcal{A}^{k-p^*}(\mathbf{B}(r)))\\ &\subseteq \mathcal{A}^{p^*}(\xi^n\mathbf{B}(r)) = \xi^n\mathcal{A}^{p^*}(\mathbf{B}(r))\\ &\subseteq \xi^{n+1}\mathbf{B}(r). \end{aligned} \tag{26}$$

Therefore, for any $k \geq np^*$, $n \in \mathbb{N}$, we have $\mathcal{A}^k(\mathbf{B}(r)) \subseteq \xi^n\mathbf{B}(r)$. Furthermore, since $\Omega_\infty = \bigoplus_{i=0}^{\infty}\mathcal{A}^i(\mathbf{S})$, we can have

$$\begin{aligned}\Omega_\infty &= \sum_{i=0}^{p^*-1}\mathcal{A}^i(\mathbf{S}) \oplus \sum_{n=1}^{\infty}\sum_{i=np^*}^{(n+1)p^*-1}\mathcal{A}^i(\mathbf{S})\\ &\subseteq \sum_{i=0}^{p^*-1}\mathcal{A}^i(\mathbf{B}(r)) \oplus \sum_{n=1}^{\infty}\sum_{i=np^*}^{(n+1)p^*-1}\mathcal{A}^i(\mathbf{B}(r))\\ &\subseteq \sum_{i=0}^{p^*-1}\mathcal{A}^i(\mathbf{B}(r)) \oplus \sum_{n=1}^{\infty}\sum_{i=np^*}^{(n+1)p^*-1}\xi^n\mathbf{B}(r)\\ &= \sum_{i=0}^{p^*-1}\mathcal{A}^i(\mathbf{B}(r)) \oplus p^*\sum_{n=1}^{\infty}\xi^n\mathbf{B}(r)\\ &= \sum_{i=0}^{p^*-1}\mathcal{A}^i(\mathbf{B}(r)) \oplus \frac{p^*\xi}{1-\xi}\mathbf{B}(r). \end{aligned} \tag{27}$$

Since p^* is a finite number, and $\mathbf{S}$ and $\mathbf{B}(r)$ are known, bounded sets, we can build the set $\mathbf{E}_0 := \sum_{i=0}^{p^*-1}\mathcal{A}^i(\mathbf{B}(r)) \oplus \frac{p^*\xi}{1-\xi}\mathbf{B}(r)$ containing the mRPI set Ω_∞. □

D. OUTER-APPROXIMATION OF THE MRPI SET WITH GIVEN PRECISION

According to Theorem 4, we can find that it needs in infinite times of iterations to obtain the mRPI set Ω_∞ of the dynamics (5), which is not realistic for obtaining the exact value of the mRPI set Ω_∞. In the following, we propose an outer-approximation method of the mRPI set with arbitrarily given precision. By combining (19) and (24), we can obtain

$$\Omega_k = \mathcal{A}^k(\Omega_0) \oplus \sum_{i=1}^{k}\mathcal{A}^{i-1}(\mathbf{S}) \subseteq \mathcal{A}^k(\Omega_0) \oplus \Omega_\infty. \tag{28}$$

Thus, the set iteration computation (17) can be terminated when there exists a $k^\dagger \in \mathbb{N}^+$ such that

$$\mathcal{A}^{k^\dagger}(\Omega_0) \subseteq \mathbb{A}_p^{n_x}(\epsilon), \tag{29}$$

with $\mathbb{A}_p^{n_x}(\epsilon) := \{x \in \mathbb{R}^{n_x} : \|x\|_p \leq \epsilon\}$ is a prior given ball with arbitrary small size. Therefore, based on (18) and (28), we can conclude that the set $\Omega_{k^\dagger}$ is not only an RPI set for the dynamics (5) but also an outer approximation of the mRPI set Ω_∞ with the precision $\mathbb{A}_p^{n_x}(\epsilon)$. That is

$$\Omega_\infty \subseteq \Omega_{k^\dagger} \subseteq \mathbb{A}_p^{n_x}(\epsilon) \oplus \Omega_\infty. \tag{30}$$

IV. COMPUTATION OF MDF IN ACTUATOR-FAULT SITUATION

This section considers computing the magnitude of MDF for the system (1) in the additive actuator-fault situation.

A. DISTURBANCE-FREE DYNAMICS WITH ADDITIVE ACTUATOR FAULTS

Let us first consider the behavior of state-estimation-error dynamics (5) with additive actuator faults in the absence of the unknown inputs w_k and the measurement noises η_k. Note that, we only consider single actuator-fault situation in order to compute the magnitude of MDF for each fault f_i, where f_i is the i-th component of f_k corresponding to the i-th actuator fault. Thus, the analysis is carried on based on the following disturbance-free dynamics:

$$\tilde{e}_{k+1}^{a,i} = (A(\theta_k) - LC(\theta_k))\tilde{e}_k^{a,i} + f_iG_i, \tag{31}$$

where G_i is the $i-th$ column of the matrix G. For simplicity, here we only consider the situation $f_i > 0$. The situation $f_i < 0$ can be handled similarly using an equivalent transformation $f_iG_i = (-f_i)(-G_i)$. Suppose that the dynamics (31) is stable, based on the results in Theorems 3 and 4, the mRPI set of the dynamics (31) can be obtained as $f_i\tilde{\mathcal{E}}_i^a$, where $\tilde{\mathcal{E}}_i^a = \bigoplus_{i=0}^{\infty}\mathcal{A}^i(G_i)$ denotes the mRPI set of the dynamics (31) in the case of $f_i = 1$.

B. HEALTHY AND ACTUATOR-FAULT RESIDUAL SETS

Combining (5) with (31), we can further derive the dynamics of state-estimation error $e_k^{a,i}$ in the single actuator-fault situation with additive uncertainties (i.e., the unknown inputs w_k and measurement noises η_k).

$$e_{k+1}^{a,i} = (A(\theta_k) - LC(\theta_k))e_k^{a,i} + Ew_k - LF\eta_k + f_iG_i,$$

with $e_k^{a,i} = e_k + \tilde{e}_k^{a,i}$ leading to the invariant set characterization:

$$\mathcal{E}_i^a = \mathcal{E} \oplus f_i\tilde{\mathcal{E}}_i^a, \tag{32}$$

where $\mathcal{E} = \Omega_\infty$ denotes the mRPI set of the dynamics (5). Since the system state vector x_k is unknown and we cannot obtain the specific value of the state estimation error e_k, we define the following residual vector corresponding to (5) in healthy situation to implement robust FD:

$$r_k = y_k - \hat{y}_k = C(\theta_k)e_k + F\eta_k. \tag{33}$$

The set version of (33) is

$$\mathcal{R} = \mathcal{C}(\mathcal{E}) \oplus F\mathbf{V}, \tag{34}$$

where $\mathcal{C}(\mathcal{E}) = \mathbf{Conv}\left\{\bigcup_{i=1}^{\mathcal{N}} C_i\mathcal{E}\right\}$. Similarly, we can get the residual signal in single actuator-fault situation:

$$\begin{aligned}r_k^{a,i} &= C(\theta_k)e_k^{a,i} + F\eta_k\\ &= C(\theta_k)e_k + F\eta_k + C(\theta_k)\tilde{e}_k^{a,i}\\ &= r_k + C(\theta_k)\tilde{e}_k^{a,i}. \end{aligned} \tag{35}$$

Furthermore, the set version of (35) can be characterized:

$$\mathcal{R}_i^a = \mathcal{R} \oplus \mathcal{C}(f_i\tilde{\mathcal{E}}_i^a) = \mathcal{R} \oplus f_i\mathcal{C}(\tilde{\mathcal{E}}_i^a). \tag{36}$$

The monitoring criterion based on invariant sets for FD needs to real-timely check whether

$$r_k \in \mathcal{R} \tag{37}$$

holds or not. If there is a violation of (37), i.e., $r_k \notin \mathcal{R}$ after a time instant $k-1$ where $r_{k-1} \in \mathcal{R}$, it indicates that the system (1) is faulty at time instant k. Otherwise, we still consider that the system (1) operates in the healthy situation. Once there is an actuator fault occurring in the system (1), based on the properties of invariant sets, we know that the residual signal r_k will converge towards the actuator-fault residual set $\mathcal{R}_i^a$. Therefore, as long as the intersection of the healthy residual set $\mathcal{R}$ and the faulty residual set $\mathcal{R}_i^a$ is empty, i.e., $\mathcal{R} \cap \mathcal{R}_i^a = \emptyset$, it can be guaranteed that the occurred and persistent actuator fault will be detected in the steady stage regardless of the specific value of the scheduling vector θ_k varying in the scheduling set Θ.

C. COMPUTATION OF MDF FOR ACTUATOR FAULTS

In this section, we propose a method to compute the magnitude of MDF by considering the constraint $\mathcal{R} \cap \mathcal{R}_i^a = \emptyset$. Thus, we formulate the following optimization problem:

$$\min_{f_i>0} f_i; \quad \mathbf{s.t.}\ \mathcal{R} \cap \mathcal{R}_i^a = \emptyset. \tag{38}$$

Unfortunately, it is difficult to directly obtain the optimal f_i owing to the complexity of the optimization problem (38). By exploiting the duality of (38), we can use Theorem 6 next to transform the optimization problem (38) into a simple LP problem to obtain the minimum of f_i. Before introducing this main result, let us recall a relevant preliminary result in Lemma 1 taken from [12].

Lemma 1: If two known polytopes $\mathcal{P}$ and $\mathcal{W}$ are given in half-space representation, i.e., $\mathcal{P} = \{x \in \mathbb{R}^n | P^x x \le P^c\}$ and $\mathcal{W} = \{x \in \mathbb{R}^n | W^x x \le W^c\}$, their Minkowski sum $\mathcal{Q} = \mathcal{P} \oplus \mathcal{W}$ can be computed by the following projection:

$$\mathcal{Q} = \left\{ r \in \mathbb{R}^n \middle| \exists\, x,\ \mathbf{s.t.} \begin{bmatrix} P^x & 0 \\ -W^x & W^x \end{bmatrix} \begin{bmatrix} x \\ r \end{bmatrix} \le \begin{bmatrix} P^c \\ W^c \end{bmatrix} \right\}.$$

Theorem 6: For the i-th actuator fault in the system (1)*, the magnitude of guaranteed MDF can be obtained by solving the following LP problem*:

$$\min_{f_i>0} \ -f_i$$
$$\mathbf{s.t.} \quad \begin{cases} Hx \le b, H_\eta y \le b_\eta, & Hx - Hz \le b, \\ H_\eta y - H_\eta t \le b_\eta, & -\tilde{H}^a z - \tilde{H}^a F t \le f_i \tilde{b}^a. \end{cases} \tag{39}$$

where $\mathbf{V} = \{\eta \in \mathbb{R}^{n_\eta} | H_\eta \eta \le b_\eta\}$, $\mathcal{C}(\mathcal{E}) = \{x \in \mathbb{R}^{n_y} | Hx \le b\}$ and $\mathcal{C}(\tilde{\mathcal{E}}_i^a) = \{x \in \mathbb{R}^{n_y} | \tilde{H}^a x \le \tilde{b}^a\}$.

Proof: Consider the dual case of (38) and let us formulate the following optimization problem using the compact convex sets $\mathcal{R}$ and $\mathcal{R}_i^a$:

$$\max_{f_i>0} f_i; \quad \mathbf{s.t.}\ \mathcal{R} \cap \mathcal{R}_i^a \neq \emptyset. \tag{40}$$

Note that, for any f_i larger than the optimizer of (40), the constraint in (38) is satisfied and thus the optimizer here represents an infimum for the optimization (38). Furthermore, the optimization problem (40) is equivalent to the optimization problem

$$\min_{f_i>0} -f_i; \quad \mathbf{s.t.}\ \mathcal{R} \cap \mathcal{R}_i^a \neq \emptyset. \tag{41}$$

Based on (34) and (36), regarding the constraint $\mathcal{R} \cap \mathcal{R}_i^a \neq \emptyset$, we have

$$\begin{aligned} &\mathcal{R} \cap \mathcal{R}_i^a \neq \emptyset \\ &\quad \Leftrightarrow \mathbf{0} \in \mathcal{R}_i^a \oplus (-\mathcal{R}) \\ &\quad \Leftrightarrow \mathbf{0} \in \mathcal{R} \oplus f_i \mathcal{C}(\tilde{\mathcal{E}}_i^a) \oplus (-\mathcal{R}) \\ &\quad \Leftrightarrow \mathbf{0} \in \mathcal{C}(\mathcal{E}) \oplus (-\mathcal{C}(\mathcal{E})) \oplus F(\mathbf{V} \oplus (-\mathbf{V})) \oplus f_i \mathcal{C}(\tilde{\mathcal{E}}_i^a). \end{aligned} \tag{42}$$

Since the sets $\mathcal{E}$ and $\tilde{\mathcal{E}}_i^a$ are the mRPI sets of the dynamics (5) and (31), respectively, both of them are known polytopes. Thus, the convex hulls $\mathcal{C}(\mathcal{E})$ and $\mathcal{C}(\tilde{\mathcal{E}}_i^a)$ are also known. For the convenience of illustration, we assume $\mathcal{C}(\mathcal{E}) = \{x \in \mathbb{R}^{n_y} | Hx \le b\}$ and $\mathcal{C}(\tilde{\mathcal{E}}_i^a) = \{x \in \mathbb{R}^{n_y} | \tilde{H}^a x \le \tilde{b}^a\}$. Then, according to Lemma 1, we have

$$\begin{aligned} &\mathcal{C}(\mathcal{E}) \oplus (-\mathcal{C}(\mathcal{E})) \\ &= \left\{ z \in \mathbb{R}^{n_y} \middle| \exists\, x,\ \mathbf{s.t.} \begin{bmatrix} H & 0 \\ H & q-H \end{bmatrix} \begin{bmatrix} x \\ z \end{bmatrix} \le \begin{bmatrix} b \\ b \end{bmatrix} \right\}, \\ &F(\mathbf{V} \oplus (-\mathbf{V})) \\ &= \left\{ \beta \in \mathbb{R}^{n_y} \middle| \exists y, t,\ \mathbf{s.t.}\ \beta = Ft, \begin{bmatrix} H_\eta & 0 \\ H_\eta & -H_\eta \end{bmatrix} \begin{bmatrix} y \\ t \end{bmatrix} \le \begin{bmatrix} b_\eta \\ b_\eta \end{bmatrix} \right\}. \end{aligned} \tag{43}$$

Furthermore, let $\mathcal{S} = \mathcal{C}(\mathcal{E}) \oplus (-\mathcal{C}(\mathcal{E})) \oplus F(\mathbf{V} \oplus (-\mathbf{V})) \oplus f_i \mathcal{C}(\tilde{\mathcal{E}}_i^a)$, which can be computed as

$$\begin{aligned} \mathcal{S} = \Bigg\{ & m \in \mathbb{R}^{n_y} \Bigg| \exists x, z, y, t, r,\ \mathbf{s.t.}\ m = z + \beta + r, \tilde{H}^a r \le f_i \tilde{b}^a \\ & \begin{bmatrix} H & 0 \\ H & -H \end{bmatrix} \begin{bmatrix} x \\ z \end{bmatrix} \le \begin{bmatrix} b \\ b \end{bmatrix}, \quad \beta = Ft, \\ & \begin{bmatrix} H_\eta & 0 \\ H_\eta & -H_\eta \end{bmatrix} \begin{bmatrix} y \\ t \end{bmatrix} \le \begin{bmatrix} b_\eta \\ b_\eta \end{bmatrix} \Bigg\} \\ = \Bigg\{ & m \in \mathbb{R}^{n_y} \Bigg| \exists x, z, y, t,\ \mathbf{s.t.} \begin{bmatrix} H & 0 \\ H & -H \end{bmatrix} \begin{bmatrix} x \\ z \end{bmatrix} \le \begin{bmatrix} b \\ b \end{bmatrix}, \\ & \beta = Ft, \begin{bmatrix} H_\eta & 0 \\ H_\eta & -H_\eta \end{bmatrix} \begin{bmatrix} y \\ t \end{bmatrix} \le \begin{bmatrix} b_\eta \\ b_\eta \end{bmatrix}, \\ & \tilde{H}^a (m - z - \beta) \le f_i \tilde{b}^a \Bigg\} \\ = \Bigg\{ & m \in \mathbb{R}^{n_y} \Bigg| \exists x, z, y, t,\ \mathbf{s.t.} \begin{bmatrix} H & 0 \\ H & -H \end{bmatrix} \begin{bmatrix} x \\ z \end{bmatrix} \le \begin{bmatrix} b \\ b \end{bmatrix}, \\ & \begin{bmatrix} H_\eta & 0 \\ H_\eta & -H_\eta \end{bmatrix} \begin{bmatrix} y \\ t \end{bmatrix} \le \begin{bmatrix} b_\eta \\ b_\eta \end{bmatrix}, \\ & \tilde{H}^a (m - z - Ft) \le f_i \tilde{b}^a \Bigg\}. \end{aligned} \tag{44}$$

Since $\mathcal{R} \cap \mathcal{R}_i^a \neq \emptyset \Leftrightarrow \mathbf{0} \in \mathcal{S}$ based on (42), by combining (44), the constraint $\mathbf{0} \in \mathcal{S}$ can lead to a series of linear constraints $Hx \le b, H_\eta y \le b_\eta, Hx - Hz \le b, H_\eta y - H_\eta t \le b_\eta$ and $-\tilde{H}^a z - \tilde{H}^a F t \le f_i \tilde{b}^a$. Finally, by minimizing $-f_i$, we obtain (39). □

Note that, Theorem 6 gives the method to compute the magnitude of guaranteed MDF no matter how the scheduling vector θ_k varies in the scheduling set Θ. We can always guarantee that the occurred fault can be detected by using the invariant set-based FD method as long as the magnitude of occurred fault is larger than that of MDF. However,

the results obtained from the optimization problem (39) may be considered conservatively since all the realizations of the scheduling vector θ_k are considered. As an alternative, using the specific value of θ_k to compute the set $C(\theta_k)\mathcal{E}$ at each time step k instead of computing the off-line convex hull $\mathcal{C}(\mathcal{E})$ in (34), we can obtain a less conservative magnitude of MDF at the price of a certain computational cost. In this case, the magnitude of MDF is dependent of the value of θ_k and we can further obtain an LP problem explicitly dependent on the scheduling vector θ_k in Theorem 7.

Theorem 7: For the i-th actuator fault in the system (1)*, given the specific value of the scheduling vector θ_k, the magnitude of MDF can be obtained by solving the following LP problem*:

$$\begin{aligned}&\min_{f_i>0} \ -f_i\\ &\text{s.t.} \begin{cases} H_{\mathcal{E}}\alpha \le b_{\mathcal{E}}, H_\eta y \le b_\eta, \\ H_{\mathcal{E}}\alpha - H_{\mathcal{E}}\xi \le b_{\mathcal{E}}, H_\eta y - H_\eta t \le b_\eta, \\ Ft = -C(\theta_k)(f_i(I - A(\theta_k) + LC(\theta_k))^{-1}G_i + \xi). \end{cases}\end{aligned}$$

Proof: The proof is similar to that of Theorem 6. Considering the space limit, we omit the detailed proof. □

V. COMPUTATION OF MDF IN SENSOR-FAULT SITUATION

In this section, we consider computing the MDF of sensor faults for the system (1) in the sensor-fault situation.

A. DISTURBANCE-FREE DYNAMICS WITH ADDITIVE SENSOR FAULTS

Here we consider the behavior of state-estimation-error dynamics (1) with additive sensor faults in the absence of the unknown inputs w_k and the measurement noises η_k. Similar to the computation of MDF for the actuator faults, we also consider single sensor-fault situation in order to compute the magnitude of MDF for each sensor fault g_i, where g_i is the i-th component of sensor fault vector g_k. Thus, the analysis is carried on the following disturbance-free dynamics with additive sensor fault:

$$\tilde{e}_{k+1}^{s,i} = (A(\theta_k) - LC(\theta_k))\tilde{e}_k^{s,i} - g_i L P_i, \tag{45}$$

where P_i is the i-th column of the matrix P. Similar to the actuator-fault situation, we only consider the case $g_i > 0$. Suppose that the dynamics (45) is stable, based on the results in Theorems 3 and 4, the mRPI set of the dynamics (45) can be obtained as $g_i\tilde{\mathcal{E}}_i^s$, where $\tilde{\mathcal{E}}_i^s = \bigoplus_{i=0}^{\infty} \mathcal{A}^i(-LP_i)$ denotes the mRPI set of the dynamics (45) in the case of $g_i = 1$.

B. SENSOR-FAULT RESIDUAL SET

Combining (5) with (45), we can further derive the dynamics of state-estimation error $e_k^{s,i}$ in the single sensor-fault situation with additive uncertainties (i.e., the unknown input w_k and measurement noise η_k).

$$e_{k+1}^{s,i} = (A(\theta_k) - LC(\theta_k))e_k^{s,i} + Ew_k - LF\eta_k - g_i L P_i, \tag{46}$$

with $e_k^{s,i} = e_k + \tilde{e}_k^{s,i}$ leading to the invariant set characterization:

$$\mathcal{E}_i^s = \mathcal{E} \oplus g_i\tilde{\mathcal{E}}_i^s, \tag{47}$$

Similarly, we can obtain the residual signal in single sensor-fault situation:

$$\begin{aligned} r_k^{s,i} &= C(\theta_k)e_k^{s,i} + F\eta_k + g_i P_i \\ &= C(\theta_k)e_k + F\eta_k + C(\theta_k)\tilde{e}_k^{s,i} + g_i P_i \\ &= r_k + C(\theta_k)\tilde{e}_k^{s,i} + g_i P_i. \end{aligned} \tag{48}$$

Furthermore, the set version of (48) can be obtained as

$$\begin{aligned} \mathcal{R}_i^s &= \mathcal{R} \oplus \mathcal{C}(g_i\tilde{\mathcal{E}}_i^s) \oplus \{g_i P_i\} \\ &= \mathcal{R} \oplus g_i\mathcal{C}(\tilde{\mathcal{E}}_i^s) \oplus \{g_i P_i\}. \end{aligned} \tag{49}$$

Furthermore, as long as the intersection of the healthy residual set $\mathcal{R}$ and the sensor-fault residual set $\mathcal{R}_i^s$ is empty, i.e., $\mathcal{R} \cap \mathcal{R}_i^s = \emptyset$, it can be guaranteed that the occurred and persistent single fault will be detected in the steady stage regardless of the specific value of the scheduling vector θ_k varying in the scheduling set Θ.

C. COMPUTATION OF MDF FOR SENSOR FAULTS

Similar to the actuator-fault situation, we can formulate the following optimization problem for sensor-fault situation:

$$\min_{g_i>0} \ -g_i; \quad \text{s.t. } \mathcal{R} \cap \mathcal{R}_i^s \neq \emptyset. \tag{50}$$

The following Theorem 8 formulates a simple LP problem to compute the MDF g_i of sensor faults.

Theorem 8: For the i-th sensor fault in the system (1)*, the magnitude of MDF g_i can be obtained by solving the following LP problem*:

$$\begin{aligned}&\min_{g_i>0} \ -g_i\\ &\text{s.t.} \begin{cases} Hx \le b, H_\eta y \le b_\eta, & Hx - Hz \le b, \\ H_\eta y - H_\eta t \le b_\eta, & -\tilde{H}^s z - \tilde{H}^s Ft \le g_i(\tilde{b}^s + \tilde{H}^s P_i). \end{cases}\end{aligned}$$

where $\mathcal{C}(\tilde{\mathcal{E}}_i^s) = \{x \in \mathbb{R}^{n_y} | \tilde{H}^s x \le \tilde{b}^s\}$.

Similarly, if we consider the specific value of θ_k, an LP problem explicitly dependent on the scheduling vector θ_k to compute the magnitude of DDF g_i is given in Theorem 9.

Theorem 9: For the i-th sensor fault in the system (1)*, given the specific value of the scheduling vector θ_k, the magnitude of MDF can be obtained by solving the following LP problem*:

$$\begin{aligned}&\min_{g_i>0} \ -g_i\\ &\text{s.t.} \begin{cases} H_{\mathcal{E}}\alpha \le b_{\mathcal{E}}, \ H_\eta y \le b_\eta, \\ H_{\mathcal{E}}\alpha - H_{\mathcal{E}}\xi \le b_{\mathcal{E}}, \ H_\eta y - H_\eta t \le b_\eta, \\ Ft = C(\theta_k)(g_i(I - A(\theta_k) + LC(\theta_k))^{-1}LP_i - \xi) - g_i P_i. \end{cases}\end{aligned}$$

where $\tilde{\mathcal{E}}_i^s = \{x \in \mathbb{R}^{n_x} | H_{\tilde{\mathcal{E}}_i^a} x \le b_{\tilde{\mathcal{E}}_i^a}\}$.

Note that, both the proofs of Theorems 8 and 9 are similar to those of the actuator-fault situation. The detailed proofs are omitted here.

VI. APPLICATION TO VEHICLE DYNAMICS MODEL

In this section, we consider the vehicle model taken from [24] to illustrate the effectiveness of the proposed method. The dynamics is given by

$$\begin{bmatrix}\dot{\beta}(t)\\ \dot{r}(t)\end{bmatrix} = \begin{bmatrix}-\frac{c_{\alpha V}+c_{\alpha H}}{mv(t)} & \frac{l_H c_{\alpha H}-l_V c_{\alpha V}}{mv^2(t)}-1\\ \frac{l_H c_{\alpha H}-l_V c_{\alpha V}}{I_z} & \frac{l_V^2 c_{\alpha V}+l_H^2 c_{\alpha H}}{I_z v(t)}\end{bmatrix}\begin{bmatrix}\beta(t)\\ r(t)\end{bmatrix} + \begin{bmatrix}\frac{c_{\alpha V}}{mv(t)}\\ \frac{l_V c_{\alpha V}}{I_z}\end{bmatrix}u(t),$$

$$\begin{bmatrix}a(t)\\ r(t)\end{bmatrix} = \begin{bmatrix}-\frac{C_{\alpha V}+C_{\alpha H}}{m} & \frac{l_H C_{\alpha H}-l_V C_{\alpha V}}{mv(t)^2}\\ 0 & 1\end{bmatrix}\begin{bmatrix}\beta(t)\\ r(t)\end{bmatrix} + \begin{bmatrix}C_{\alpha V}\\ 0\end{bmatrix}u(t),$$

where $\beta(t)$ denotes the side slip angle, $r(t)$ the yaw rate, u the relative steering wheel angle and $a(t)$ the lateral acceleration. The remaining definitions and values of all the involved parameters are displayed in Table 1.

TABLE 1. Parameters of vehicle model.

Variable	Value	Comments
m	$1621kg$	Vehicle total mass
I_z	$1975kg\cdot m^2$	Moment of inertial about the z-axis
$c_{\alpha V}$	$57117N/rad$	Front axle tire cornering stiffness
$c_{\alpha H}$	$81396N/rad$	Rear axle tire cornering stiffness
l_V	$1.15m$	Distance from C.G. to front axle
l_H	$1.38m$	Distance from C.G. to rear axle
v	$[2,4]m/s$	Vehicle longitudinal velocity

We discretize the primitive continuous-time model with a sampling period $T_d = 0.1s$ by using the first-order Euler difference method and define two scheduling variables $\theta_k(1)=\frac{1}{v}$ and $\theta_k(2)=\frac{1}{v^2}$. Then, the nonlinear vehicle model can be equivalently transformed into a discrete-time LPV model:

$$\begin{bmatrix}\beta_{k+1}\\ r_{k+1}\end{bmatrix} = \begin{bmatrix}1-T_d\frac{C_{\alpha V}+C_{\alpha H}}{m}\theta_k(1) & T_d\frac{l_H C_{\alpha H}-l_V C_{\alpha V}}{m}\theta_k(2)-T_d\\ T_d\frac{l_H C_{\alpha H}-l_V C_{\alpha V}}{I_z} & 1+T_d\frac{l_V^2 C_{\alpha V}+l_H^2 C_{\alpha H}}{I_z}\theta_k(1)\end{bmatrix} \times\begin{bmatrix}\beta_k\\ r_k\end{bmatrix} + \begin{bmatrix}T_d\frac{C_{\alpha V}}{m}\theta_k(1)\\ T_d\frac{l_V C_{\alpha V}}{I_z}\end{bmatrix}u_k,$$

$$\begin{bmatrix}a_k\\ r_k\end{bmatrix} = \begin{bmatrix}-\frac{C_{\alpha V}+C_{\alpha H}}{m} & \frac{l_H C_{\alpha H}-l_V C_{\alpha V}}{m\theta_k(2)}\\ 0 & 1\end{bmatrix}\begin{bmatrix}\beta_k\\ r_k\end{bmatrix}+\begin{bmatrix}C_{\alpha V}\\ 0\end{bmatrix}u_k.$$

In this example, the speed $v(t)$ varies between $2m/s$ and $4m/s$. Since $v(t)$ is bounded, $\theta_k(1)$ and $\theta_k(2)$ are also bounded.

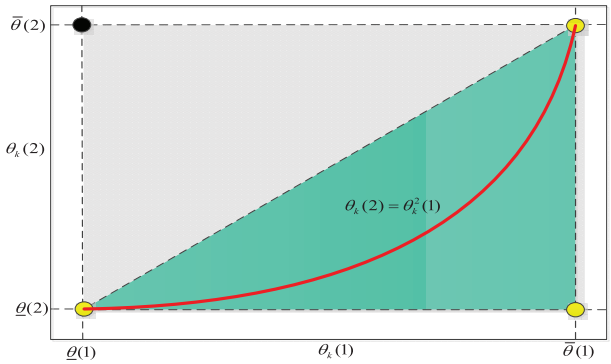

FIGURE 1. Vertex reduction.

This implies that a polytope bounding the vector composed of these two scheduling variables can be obtained and it has four vertices. Meanwhile, by using the vertices, the vehicle model can be transformed into a polytopic LPV form. Furthermore, since $\theta_k(1)$ and $\theta_k(2)$ have an explicit mathematical relationship as shown in Figure 1, i.e., $\theta_k(2)=\theta_k^2(1)$,

The number of the vertices of the obtained LPV model can be reduced to three, i.e., $\mathcal{N}=3$ (see [24] for more details). Thus, the bounding set of the scheduling vector θ_k is obtained as

$$\begin{aligned}\Theta &= \mathbf{Conv}\left\{\begin{bmatrix}\underline{\theta}(1)\\ \underline{\theta}(2)\end{bmatrix},\begin{bmatrix}\bar{\theta}(1)\\ \underline{\theta}(2)\end{bmatrix},\begin{bmatrix}\bar{\theta}(1)\\ \bar{\theta}(2)\end{bmatrix}\right\}\\ &= \mathbf{Conv}\left\{\begin{bmatrix}0.25\\ 0.0625\end{bmatrix},\begin{bmatrix}0.5\\ 0.0625\end{bmatrix},\begin{bmatrix}0.5\\ 0.25\end{bmatrix}\right\}.\end{aligned}$$

Furthermore, the bounding sets of unknown inputs w_k and measurement noises η_k are designed as $\mathbf{W} = \{w \in \mathbb{R}^2 | \|w\|_\infty \le 0.05\}$ and $\mathbf{V}=\{\eta\in\mathbb{R}^2|\|\eta\|_\infty\le 0.05\}$, whose distribution matrices E and F are respectively given by

$$E=\begin{bmatrix}0.6324 & 0.2785\\ 0.0975 & 0.5469\end{bmatrix},\quad F=\begin{bmatrix}0.9572 & 0.8003\\ 0.4854 & 0.1419\end{bmatrix}.$$

In this example, we consider two additive actuator faults $\begin{bmatrix}f_1 & f_2\end{bmatrix}^T$ and two additive sensor faults $\begin{bmatrix}g_1 & g_2\end{bmatrix}^T$, whose distribution matrices are respectively designed as

$$G=\begin{bmatrix}0.8147 & 0.1270\\ 0.9058 & 0.9134\end{bmatrix},\quad P=\begin{bmatrix}0.9575 & 0.1576\\ 0.9649 & 0.9706\end{bmatrix}.$$

The gain matrix L of the designed FD observer (3) is given as

$$L=\begin{bmatrix}-0.0178 & 0.0400\\ -0.0028 & 0.6386\end{bmatrix}.$$

Based on Theorem 1, we can solve the LMIs (7) and obtain the proper parametric matrices to verify the poly-quadratical stability of the dynamics (5) using YALMIP [13]:

$$S_1=\begin{bmatrix}9.0061 & 0.0152\\ 0.0152 & 9.1924\end{bmatrix},\quad S_2=\begin{bmatrix}7.2147 & 0.0020\\ 0.0020 & 6.7395\end{bmatrix},$$
$$S_3=\begin{bmatrix}7.2531 & 0.5289\\ 0.5289 & 6.6162\end{bmatrix},\quad M_1=\begin{bmatrix}8.6153 & 0.0036\\ 0.0082 & 8.8690\end{bmatrix},$$
$$M_2=\begin{bmatrix}7.0225 & -0.0003\\ -0.0165 & 6.6299\end{bmatrix},\quad M_3=\begin{bmatrix}7.0499 & 0.5015\\ 0.5164 & 6.4982\end{bmatrix}.$$

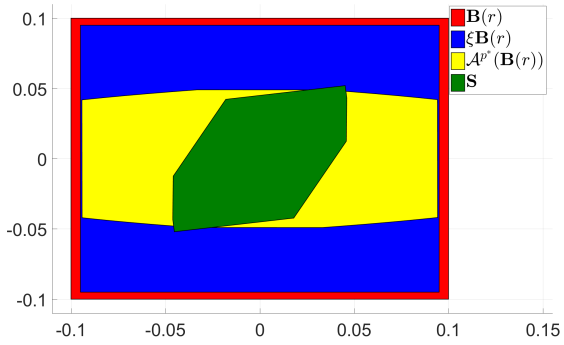

FIGURE 2. Construction of $\mathbf{E_0}$.

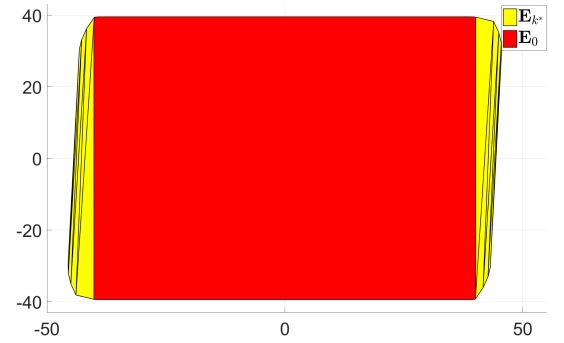

FIGURE 3. Computation of initial RPI set $\mathbf{E}_{k^*}$.

We first consider the construction of the initial set $\mathbf{E}_0$ in the healthy situation and the related sets are shown in Figure 2. The green region denotes the set $\mathbf{S} = E\mathbf{W} \oplus (-LF)\mathbf{V}$. The red region denotes the box $\mathbf{B}(r) = \{x \in \mathbb{R}^2 : \|x\|_\infty \leq 0.1\}$ containing the set $\mathbf{S}$. Furthermore, we can find that the yellow region is contained in the blue region, i.e., $\mathcal{A}^{p^*}(\mathbf{B}(r)) \subseteq \xi\mathbf{B}(r)$ with $\xi = 0.95$ and $p^* = 20$. Thus, we can further implement the construction of $\mathbf{E}_0$ using (25) in Theorem 5.

By iterating (11) in Theorem 3, we can compute the initial RPI set $\mathbf{E}_{k^*}$ with a number of $k^* = 8$ iterations. The whole iterative procedure computing $\mathbf{E}_{k^*}$ from the initial set $\mathbf{E}_0$ is displayed in Figure 3.

Then, by using a shrinking process with the initial set $\mathbf{E}_{k^*}$ based on Theorem 4, we can obtain a sequence of outer-approximations of the mRPI set $\mathcal{E}$, which are shown in Figure 4. We can find that these outer-approximations of the mRPI set $\mathcal{E}$ are also positively invariant. After 329 iterations, the outer-approximations converge to a suitable outer invariant approximation of the mRPI set $\mathcal{E}$ with the approximating precision $\epsilon = 0.001$.

For the scheduling vector θ_k varying in the set Θ, we consider computing the magnitude of MDF f_1, f_2 and g_1, g_2 based on Theorems 6 and 8, respectively. The set separation results between the healthy and faulty residual sets with respect to MDF f_1, f_2, g_1 and g_2 are shown in Figure 5. The corresponding magnitudes of MDF are $f_1 = 1.1741, f_2 = 1.1643$, $g_1 = 3.7427$ and $g_2 = 3.6915$. Thus, for any actuator or sensor fault, as long as their magnitudes are larger than the corresponding thresholds, we can guarantee the detection of

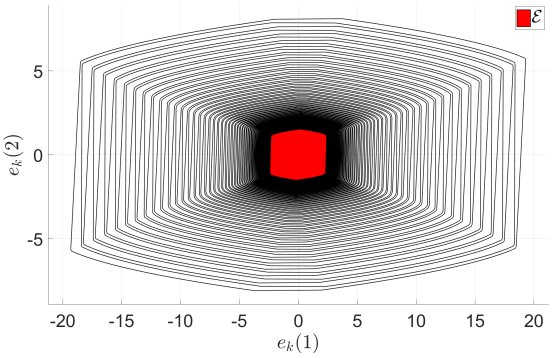

FIGURE 4. Shrinking process.

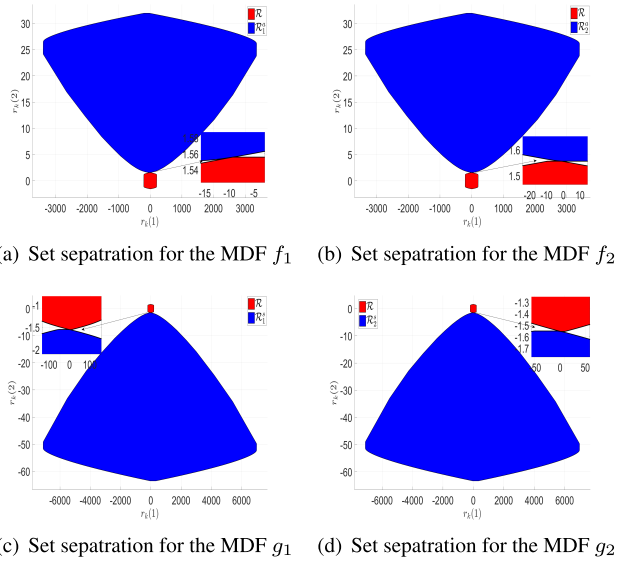

(a) Set sepatration for the MDF f_1 (b) Set sepatration for the MDF f_2

(c) Set sepatration for the MDF g_1 (d) Set sepatration for the MDF g_2

FIGURE 5. The set-separation results between the healthy and faulty residual sets w.r.t MDF f_1, f_2, g_1 and g_2 for any $\theta_k \in \Theta$.

a persistent fault regardless of the value of the scheduling vector θ_k varying in Θ.

Since the varying range of the scheduling vector θ_k can affect the magnitude of MDF, we can lower the conservatism of results on the magnitude of MDF by decreasing the varying range of the scheduling vector θ_k. In this example, since the scheduling vector θ_k is directly dependent on the vehicle speed v, we use the variation of v to characterize the varying range of the scheduling vector θ_k. The magnitudes of MDF for the actuator and sensor faults w.r.t different varying ranges of v are displayed in Table 2. Furthermore, for the specific value of θ_k, we can also compute the corresponding magnitude of MDF for actuator and sensor faults based on Theorems 7 and 9, respectively.

For the clarity of display and illustration, we show the case of specific value of θ_k and results of Table 2 in Figure 6. We take Figure 6(a) as an example to illustrate the results on the magnitude of MDF f_1 w.r.t different varying ranges of v. The purple line in Figure 6(a) denotes the magnitudes of MDF for specific values of speed v, which is plotted by using an interpolation method to compute a magnitude of MDF

TABLE 2. The magnitude of MDF for actuator and sensor faults w.r.t different varying ranges of v.

Varying range of v	f_1	f_2	g_1	g_2
$v \in [2,4]m/s$	1.1741	1.1643	3.7427	3.6915
$v \in [2,3]m/s$	0.8318	0.8238	1.9703	1.9472
$v \in [3,4]m/s$	0.1998	0.1978	0.6368	0.6282
$v \in [2,2.5]m/s$	0.5553	0.5479	1.0901	1.0784
$v \in [2.5,3]m/s$	0.2025	0.2005	0.4803	0.4747
$v \in [3,3.5]m/s$	0.1746	0.1729	0.4853	0.4792
$v \in [3.5,4]m/s$	0.1670	0.1654	0.5328	0.5257

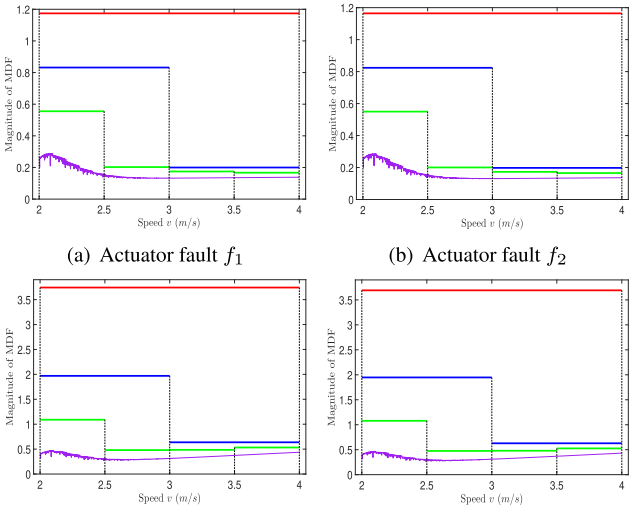

(a) Actuator fault f_1 (b) Actuator fault f_2

(c) Sensor fault g_1 (d) Sensor fault g_2

FIGURE 6. The different magnitudes of MDF f_1, f_2, g_1 and g_2 w.r.t different varying ranges of v.

with a step increment of $0.001m/s$ from $2m/s$ to $4m/s$. The four green lines from left to right represent the magnitudes of MDF f_1 when $v \in [2, 2.5]m/s$, $v \in [2.5, 3]m/s$, $v \in [3, 3.5]m/s$ and $v \in [3.5, 4]m/s$, respectively. It can be found that in each small interval (i.e., $[2, 2.5]m/s$, $[2.5, 3]m/s$, $[3, 3.5]m/s$ or $[3.5, 4]m/s$), since the speed v has a larger varying range for the green line, the purple line is always below the green line, which exactly matches the theoretic analysis that the conservatism of results on MDF can be lowered by decreasing the varying range of the scheduling vector θ_k. Similarly, the two blue lines from left to right denote the magnitudes of MDF f_1 when $v \in [2, 3]m/s$ and $v \in [3, 4]m/s$, respectively. Since the two small intervals $[2, 2.5]m/s$ and $[2.5, 3]m/s$ are both contained in the larger interval $[2, 3]m/s$, the corresponding green lines and purple line are all below the blue line, which implies that the result of MDF f_1 for the blue line has a higher conservatism. The red line corresponds the magnitude of MDF f_1 when $v \in [2, 4]m/s$, whose result is the most conservative since all possible values of speed v are considered. It can be found that all other blue lines, green lines and purple line are below the red line. For the remaining Figures 6(b), 6(c) and 6(d), we can conduct the similar analysis and obtain the similar results. Based on the above analysis, it can be found that if we know more information (i.e., the punctual value) on the scheduling vector θ_k, we can decrease the conservatism of the magnitude of MDF as expected.

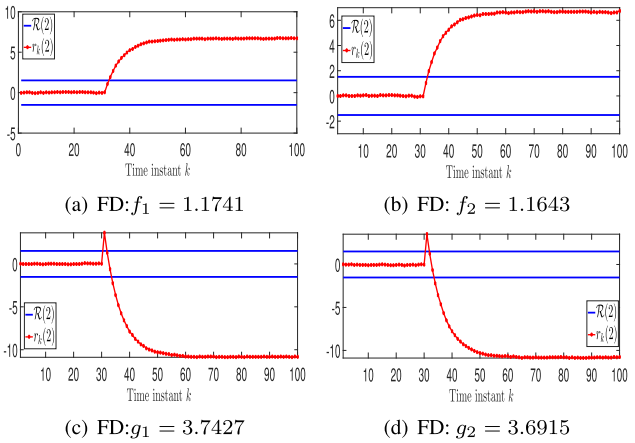

(a) FD:$f_1 = 1.1741$ (b) FD: $f_2 = 1.1643$

(c) FD:$g_1 = 3.7427$ (d) FD: $g_2 = 3.6915$

FIGURE 7. The results of FD for the MDF f_1, f_2, g_1 and g_2 when $v \in [2, 4]m/s$.

Furthermore, the results of FD on the MDF f_1, f_2, g_1 and g_2 when $v \in [2, 4]m/s$ are shown in Figure 7. We take Figure 7(a) as an example to illustrate the results of FD for the MDF $f_1 = 1.1741$ when $v \in [2, 4]m/s$. For the convenience of display, we consider drawing the interval hull (the two blue lines) of the healthy residual set $\mathcal{R}$ and only the second components of $\mathcal{R}$ and r_k are shown in the plot. We consider the following fault scenario: from $k = 0$ to $k = 30$, the system operates in the health situation. From $k = 31$ to $k = 100$, we inject a fault f_1 into the system. Then, the results of online FD are shown in Figure 7(a). We can find that from $k = 31$ to $k = 32$, the residual r_k is contained in the healthy residual set $\mathcal{R}$ and the detection cannot be triggered due to the transitory. From $k = 33$ to $k = 100$, the residual r_k is no longer contained in $\mathcal{R}$ and the fault f_1 is detected by using our proposed method. Furthermore, similar analysis can be conducted in Figures 7(b), 7(c) and 7(d) for the results of FD on the remaining faults f_2, g_1 and g_2.

VII. CONCLUSION

This paper characterizes the MDF for perturbed discrete-time LPV systems affected by additive faults using the invariant set theory. The main contribution is threefold. First, we propose a novel two-stage set computation method for state estimation error dynamics with LPV form, which does not need to satisfy the sufficient condition that there must exists a common quadratic Lyapunov function for all the vertex matrices of the dynamics. Furthermore, we can obtain the healthy and faulty residual sets based on such approximations of the mRPI set. Second, by considering the duality of guaranteed MDF problem, we transform the complex set-separation constraint into a simple and tractable LP problem to compute the magnitude of MDF. Third, the conservatism of results on the magnitude of MDF can be decreased if more information (i.e., the punctual values or smaller varying ranges) on the scheduling vector θ_k can be obtained. In the future, we aim to extend these results to the active fault diagnosis and

fault-tolerant control fields, with applications in areas such as robotics, biotechnology, process automation.

REFERENCES

[1] B. Barmish and J. Sankaran, "The propagation of parametric uncertainty via polytopes," *IEEE Trans. Autom. Control*, vol. AC-24, no. 2, pp. 346–349, Apr. 1979.
[2] F. Blanchini, "Set invariance in control," *Automatica*, vol. 35, no. 11, pp. 1747–1767, Nov. 1999.
[3] M. Blanke, M. Kinnaert, J. Lunze, and M. Staroswiecki, *Diagnosis and Fault-Tolerant Control*. Berlin, Germany: Springer-Verlag, 2006.
[4] J. Bokor, Z. Szabo, and G. Stikkel, "Failure detection for quasi LPV systems," in *Proc. 41th IEEE Conf. Decis. Control*, Las Vegas, NV, USA, Dec. 2002, pp. 3318–3323.
[5] J. Daafouz and J. Bernussou, "Parameter dependent Lyapunov functions for discrete time systems with time varying parametric uncertainties," *Syst. Control Lett.*, vol. 43, no. 5, pp. 355–399, Aug. 2001.
[6] V. M. de Oca, V. Puig, and J. Blesa, "Robust fault detection based on adaptive threshold generation using interval LPV observers," *Int. J. Adapt. Control Signal Process.*, vol. 26, no. 3, pp. 258–283, 2012.
[7] P. García and K. Ampountolas, "Robust disturbance rejection by the attractive ellipsoid method—Part II: Discrete-time systems," *IFAC-PapersOnLine*, vol. 51, no. 32, pp. 93–98, 2018.
[8] M. S. Ghasemi and A. A. Afzalian, "Invariant convex approximations of the minimal robust invariant set for linear difference inclusions," *Nonlinear Anal., Hybrid Syst.*, vol. 27, pp. 289–297, Feb. 2018.
[9] H. Khalil, *Nonlinear Systems*. New York, NY, USA: Prentice-Hall, 2002.
[10] E. Kofman, H. Haimovich, and M. M. Seron, "A systematic method to obtain ultimate bounds for perturbed systems," *Int. J. Control*, vol. 80, no. 2, pp. 167–178, 2007.
[11] K. I. Kouramas, S. V. Raković, E. C. Kerrigan, J. C. Allwright, and D. Q. Mayne, "On the minimal robust positively invariant set for linear difference inclusions," in *Proc. 44th IEEE Conf. Decis. Control, Eur. Control Conf.*, Seville, Spain, Dec. 2005, pp. 2296–2301.
[12] M. Kvasnica. (2005). *Minkowski Addition of Convex Polytopes*. [Online]. Available: http://www.researchgate.net/publication/249915078_Minkowski_addition_of_convex_polytopes
[13] J. Löfberg, "YALMIP: A toolbox for modeling and optimization in MATLAB," in *Proc. IEEE Int. Conf. Robot. Automat.*, Taipei, Taiwan, Sep. 2004, pp. 284–289.
[14] J. J. Martinez, N. Loukkas, and N. Meslem, "H-infinity set-membership observer design for discrete-time LPV systems," *Int. J. Control*, pp. 1–25, Nov. 2018. doi: 10.1080/00207179.2018.1554910.
[15] A. P. Molchanov and Y. S. Pyatnitskiy, "Criteria of asymptotic stability of differential and difference inclusions encountered in control theory," *Syst. Control Lett.*, vol. 13, no. 1, pp. 59–64, 1989.
[16] H.-N. Nguyen, S. Olaru, P.-O. Gutman, and M. Hovd, "Constrained control of uncertain, time-varying linear discrete-time systems subject to bounded disturbances," *IEEE Trans. Autom. Control*, vol. 60, no. 3, pp. 831–836, Mar. 2015.
[17] S. Olaru, J. A. De Doná, M. M. Seron, and F. Stoican, "Positive invariant sets for fault tolerant multisensor control schemes," *Int. J. Control*, vol. 83, no. 12, pp. 2622–2640, 2010.
[18] M. Rodrigues, M. Sahnoun, D. Theilliol, and J.-C. Ponsart, "Sensor fault detection and isolation filter for polytopic LPV systems: A winding machine application," *J. Process Control*, vol. 23, no. 6, pp. 805–816, 2013.
[19] M. M. Seron and J. A. De Doná, "Robust fault estimation and compensation for LPV systems under actuator and sensor faults," *Automatica*, vol. 52, pp. 294–301, Feb. 2015.
[20] M. M. Seron, J. A. De Doná, and J. J. Martínez, "Invariant set approach to actuator fault tolerant control," *IFAC Proc. Volumes*, vol. 42, no. 8, pp. 1605–1610, 2009.
[21] M. M. Seron, J. A. D. Dona, and S. Olaru, "Fault tolerant control allowing sensor healthy-to-faulty and faulty-to-healthy transitions," *IEEE Trans. Autom. Control*, vol. 57, no. 7, pp. 1657–1669, Jul. 2012.
[22] J. S. Shamma and M. Athans, "Gain scheduling: Potential hazards and possible remedies," *IEEE Control Syst. Mag.*, vol. 12, no. 3, pp. 101–107, Jun. 1992.
[23] A. Varga, *Solving Fault Diagnosis Problems: Linear Synthesis Techniques*. Berlin, Germany: Springer, 2017.
[24] S. Varrier, D. Koenig, and J. J. Martinez, "Robust fault detection for uncertain unknown inputs LPV system," *Control Eng. Pract.*, vol. 22, pp. 125–134, Jan. 2014.
[25] F. Xu, "Diagnosis and fault-tolerant control using set-based methods," Ph.D. dissertation, Inst. Org. Control Syst. Ind., Polytech. Univ. Catalonia, Barcelona, Spain, 2014.

JUNBO TAN received the bachelor's degree from the Department of Management and Engineering, Nanjing University, Nanjing, China, in 2013, and the master's degree from the Department of Automation, Tsinghua University, Beijing, China, in 2016 where he is currently pursuing the Ph.D. degree with the Navigation and Control Research Center. His research interests include fault diagnosis, linear parameter-varying systems, and fault-tolerant control.

SORIN OLARU is currently a Professor with the CentraleSupélec, Paris-Saclay University, France, and a member of the CNRS Laboratory of Signals and Systems, Paris-Saclay University. His research interests include encompassing the optimization-based control design, set-theoretic characterization of constrained dynamical systems as well as the numerical methods in optimization and control. He is currently involved in research projects related to embedded predictive control, fault tolerant control and network control (time-delay) systems.

MONICA ROMAN is currently a Professor with the Department of Automatic Control and Electronics, Faculty of Automation, Computers and Electronics, University of Craiova, and a member of the Laboratory of Modeling, Identification and Control of Bioprocesses (MICBIO), INCESA. Her main research interests include modeling and simulation of linear and nonlinear systems, bond graph methodology and its applications, and identification and control of chemical reaction-based processes.

FENG XU received the bachelor's degree (Hons.) in measurement and control technology and instruments from Northwestern Polytechnical University (NWPU), Xi'an, China, in July 2010, and the Ph.D. degree (Hons.) in automatic control from the Technical University of Catalonia (UPC), Barcelona, Spain, in November 2014. From January to April 2014, he was a Visiting Ph.D. student with the Centrale-Supélec, Paris, France. Since March 2015, he has been an Assistant Professor with Tsinghua University, China. His research interests include fault diagnosis, fault-tolerant control, and model predictive control and their applications.

BIN LIANG received the bachelor's and master's degrees from the Honors College, Northwestern Polytechnical University, Xi'an, China, in 1989 and 1991, respectively, and the Ph.D. degree from the Department of Precision Instrument, Tsinghua University, Beijing, China, in 1994. From 1994 to 2003, he was a Postdoctoral Researcher, an Associate Researcher, and a Researcher with the China Academy of Space Technology. From 2003 to 2007, he was a Researcher and an Assistant Chief Engineer with China Aerospace Science and Technology Corporation. Since 2007, he has been a Professor with the Department of Automation, Tsinghua University. He has authored and coauthored over 100 articles in international journals and conference proceedings. His research interest includes modeling and control of dynamic systems and their applications to space robots and satellites.